ACS OMEGA

Open Access

http://pubs.acs.org/journal/acsodf

Article

Study on the Phase Behavior Simulation Method of High-Salinity Reservoirs

Zhongxin Ren,* Jianjun Li, Hongfei Yuan, Chunxi Ai, Hui He, and Ken Qin

Cite This: *ACS Omega* 2024, 9, 20176−20184

Read Online

ACCESS | Metrics & More | Article Recommendations

ABSTRACT: The presence of salinity affects the accuracy of existing correlations used in the equation of state. Moreover, the variation of salinity is often ignored in the systematic analysis of the phase diagram, resulting in a large error in the final calculation result. It is obvious that the conventional phase equilibrium calculation is not applicable in a high-salinity reservoir. By introducing the hydrocarbon−brine binary interaction coefficient and α-function, combined with the definition of salinity, and considering the variation of salinity under different pressure and temperature conditions, a more perfect phase equilibrium calculation model was established. The complete phase diagram was drawn, and the calculation results of salinity distribution are obtained. The effect of the mole percentage of water and salt content on the phase behavior was simulated. Finally, the phase distribution simulation is carried out based on the measured data. The phase state and salinity variation law of a high-salinity reservoir are obtained. According to the fluid composition of different periods, the real phase state of the high-salinity reservoir can be monitored in real time. It can provide a theoretical basis for the gas reservoir development and the dynamic evaluation of gas storage injection and production with a hydrocarbon−brine two-phase system.

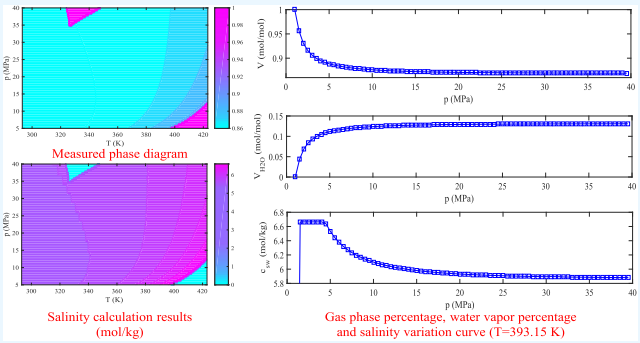

INTRODUCTION

In the process of oil and gas processing and numerical simulation of oil and gas reservoirs, a large number of hydrocarbon−water mixed systems are often involved.[1,2] The separation of components from the mixture is particularly important. Accurate phase equilibrium calculation and physical parameter prediction have gradually become the basis and key.

For aqueous systems, the three-phase flash calculation method is mostly used. Li[3] and Okuno[4] simplified the binary interaction coefficient in the three-phase flash calculation. Based on the quadratic expression, the binary interaction coefficient is decomposed into two parameters to improve the flash calculation efficiency. Based on this, Mohebbinia et al.[5] developed a four-phase flash calculation algorithm and applied the modified PR equation of state to aqueous mixtures. Comparing with the traditional flash calculation method, the speed of flash calculation by using the simplified method is significantly improved. The results show that the saturation pressure changes significantly after addition of water into the hydrocarbon system. Zhao[6] used the improved Wong−Sandler mixing rule and nonrandom two-liquid (NRTL) model to propose a simple and reliable phase model for component reservoir simulation and conducted the flash calculations for the gas−water system under reservoir temperature and pressure. The model can maintain good stability in dealing with strong polar fluid and hydrocarbon fluid systems. Wyczesany[7] used different models to calculate the vapor−liquid equilibrium for low pressure and high pressure separately and compared their accuracy.

In order to ensure the stability of the calculation, the algorithm processing method is proposed in many cases.[8−11]

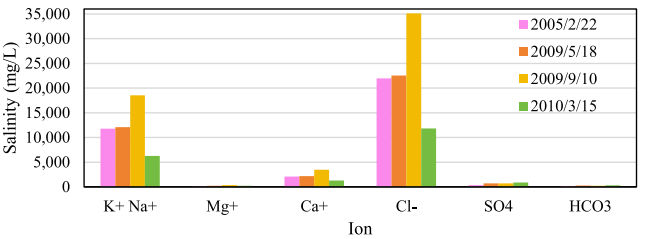

Figure 1. Water sampling analysis results.

Received: January 11, 2024
Revised: March 14, 2024
Accepted: March 18, 2024
Published: April 24, 2024

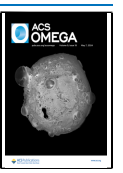

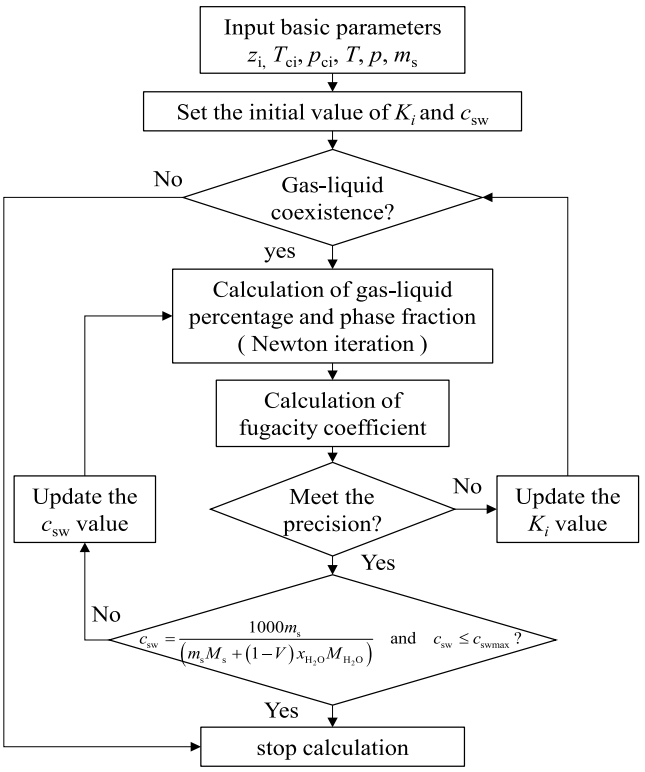

Figure 2. Phase equilibrium calculation flowchart.

Table 1. Maximum NaCl Solubility in 100 g of Water

T (°C)	0	10	20	25	30	40
NaCl (g)	35.65	35.72	35.89	35.96	36.09	36.37
T (°C)	50	60	70	80	90	100
NaCl (g)	36.69	37.04	37.46	37.93	38.47	38.99

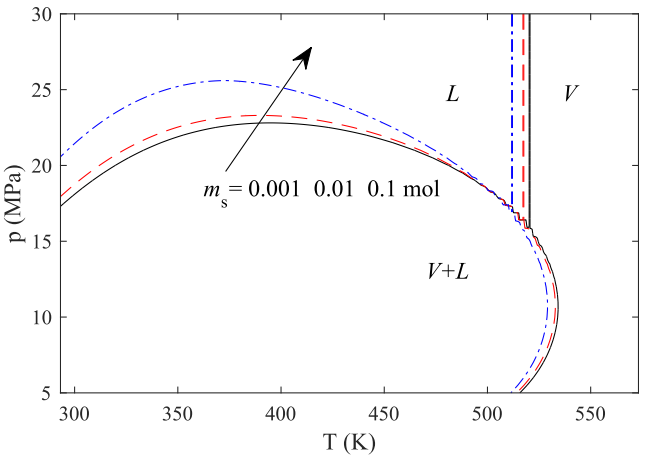

Figure 3. Phase diagram at different salt contents (C_1, C_{10}, and H_2O system).

Hinojosa-Gómez et al.[12] took into account the continuity of the phase boundary and combined with the inverse barrier function to solve the gas−liquid−liquid three-phase equilibrium calculation model, which improved the stability of the algorithm. Lindeloff and Michelsen[13] proposed an algorithm that can trace the two- and three-phase boundaries encountered, and a relatively complete phase diagram is obtained. Wang et al.[14] proposed an artificial neural network (ANN) model to accelerate the flash simulation process. Zhao et al.[15] and Michelsen[16] proved that the use of simplified variables can greatly accelerate the solution of the continuous replacement iteration problem of two-phase flash and improve the computational performance by comparing with the traditional flash calculation model. Ebadi et al.[17] combined the MBF algorithm with the flash calculation model to quickly determine the saturation pressure.

With the deepening of research, some scholars[18−21] have proposed four-phase and multiphase flash calculation methods. Under formation conditions, Neshat et al.,[22] Achour et al.,[23] Wang et al.,[24] and Sandoval et al.[25] carried outgas−liquid flash calculations through considering the influence of the capillary force. The modified method greatly improves the accuracy of the calculation considering the capillarity effect.[26] In addition, the calculation of phase equilibrium is also well applied under high-pressure conditions such as frozen soil and seabed.[27]

At present, a variety of calculation methods for phase equilibrium have been proposed,[28−31] and some of the above theories have been implemented in software.[32] However, most of the above studies did not consider the influence of salinity on phase distribution, and there was a lack of systematic analysis of the phase diagram for brine systems. In a few studies, only the salinity is regarded as a constant.[5] In the process of actual gas reservoir exploitation, salt deposit is easy to occur in the near-wellbore area, causing the change of formation water salinity.[33−35] The salinity is always affected by reservoir temperature and pressure. Through field fluid sampling, the ion concentration in different periods of a well in the Wen 23 gas field is shown in Figure 1; it was found that the main component of salt was NaCl. In order to clearly characterize the phase characteristics, only the gas and liquid phases are distinguished. Therefore, considering the variation of salinity under reservoir conditions, the phase equilibrium calculation model of the hydrocarbon−brine system was established. The phase behavior under different salt contents was simulated. The calculation results and distribution law of salinity are given. Finally, the conclusions of this work are presented.

METHODOLOGY

Phase Equilibrium Model. The PR-state equation is widely used in phase equilibrium calculation, and its expression is

$$p = \frac{RT}{V-b} - \frac{a\alpha}{V(V+b)+b(V-b)} \quad (1)$$

where

$$a = 0.45724\frac{R^2T_c^2}{p_c},\ b = 0.07780\frac{RT_c}{p_c},\ \alpha = [1 + m(1-\sqrt{T_r})]^2,\ T_r = \frac{T}{T_c}$$

$$m = 0.3796 + 1.54226\omega - 0.2699\omega^2$$

$$m = 0.379642 + 1.48503\omega - 0.1644\omega^2 + 0.016667\omega^3 (\omega > 0.49)$$

The PR equation of state is expressed by the compression factor

https://doi.org/10.1021/acsomega.4c00223
ACS Omega 2024, 9, 20176−20184

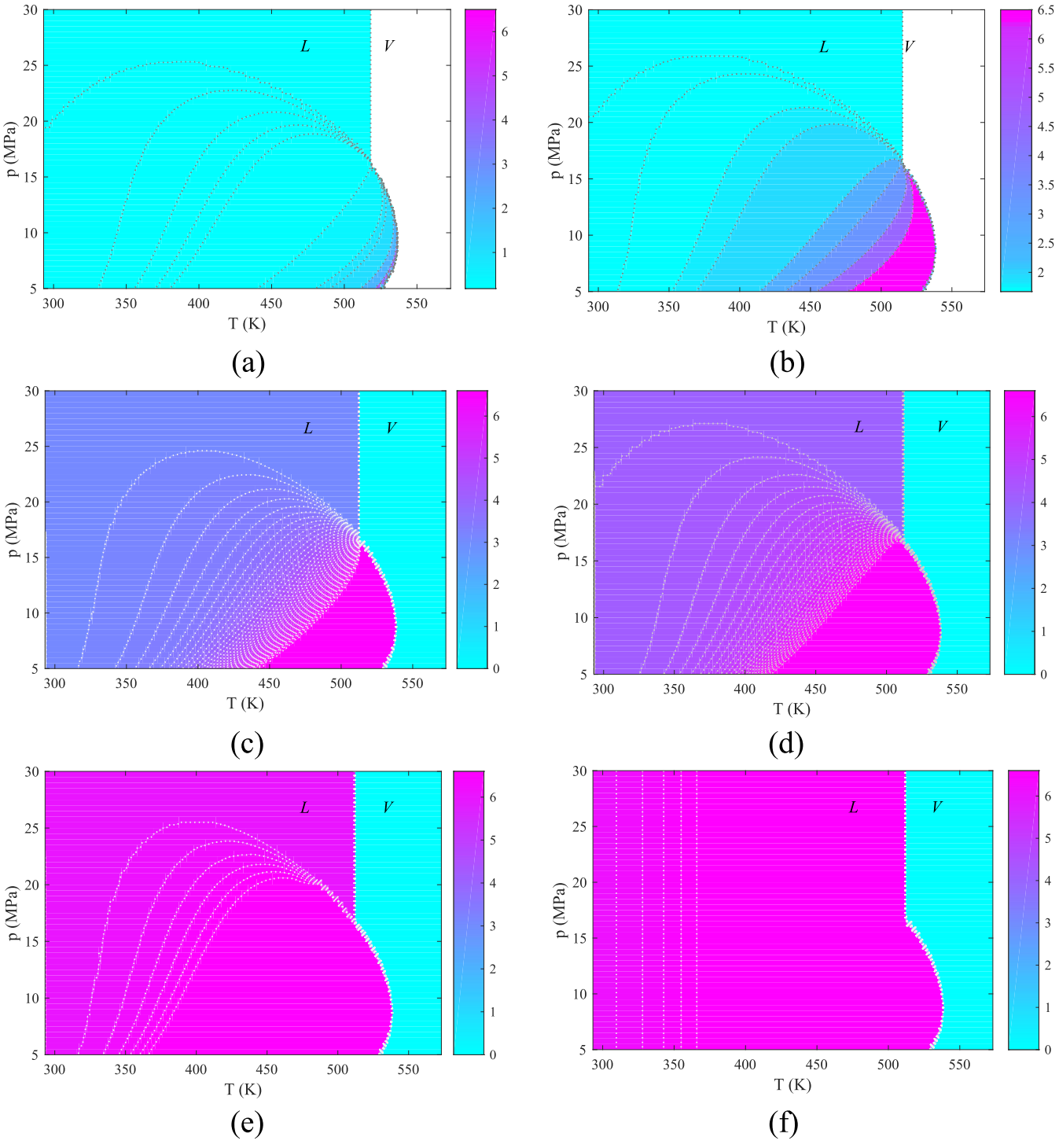

Figure 4. Salinity distribution result (mol/kg). The corresponding salt content m_s in (a–f) is 0.001, 0.01, 0.02, 0.03, 0.05, and 0.1 mol, respectively.

$$Z^3 + (B-1)Z^2 + (A - 3B^2 - 2B)Z - (AB - B^2 - B^3) = 0 \quad (2)$$

The gas- or liquid-phase fugacity coefficient expression is

$$\ln \varphi_i = \frac{b_i(Z-1)}{b_m} - \ln(Z-B) - \frac{A}{2\sqrt{2}B}\left[\frac{2\psi_i}{(a\alpha)_m} - \frac{b_i}{b_m}\right] \cdot \ln\frac{Z + (1+\sqrt{2})B}{Z + (1-\sqrt{2})B} \quad (3)$$

where

$$A = \frac{(a\alpha)_m p}{(RT)^2}, \quad B = \frac{b_m p}{RT}, \quad Z = \frac{pV}{RT}$$

For the gas phase

$$(a\alpha)_m = \sum_i \sum_j [y_i y_j \sqrt{a_i a_j \alpha_i \alpha_j} \cdot (1 - k_{ij})], \quad b_m = \sum_i y_i b_i, \quad \psi_i = \sum_j [y_j \sqrt{a_i a_j \alpha_i \alpha_j}(1 - k_{ij})]$$

https://doi.org/10.1021/acsomega.4c00223
ACS Omega 2024, 9, 20176−20184

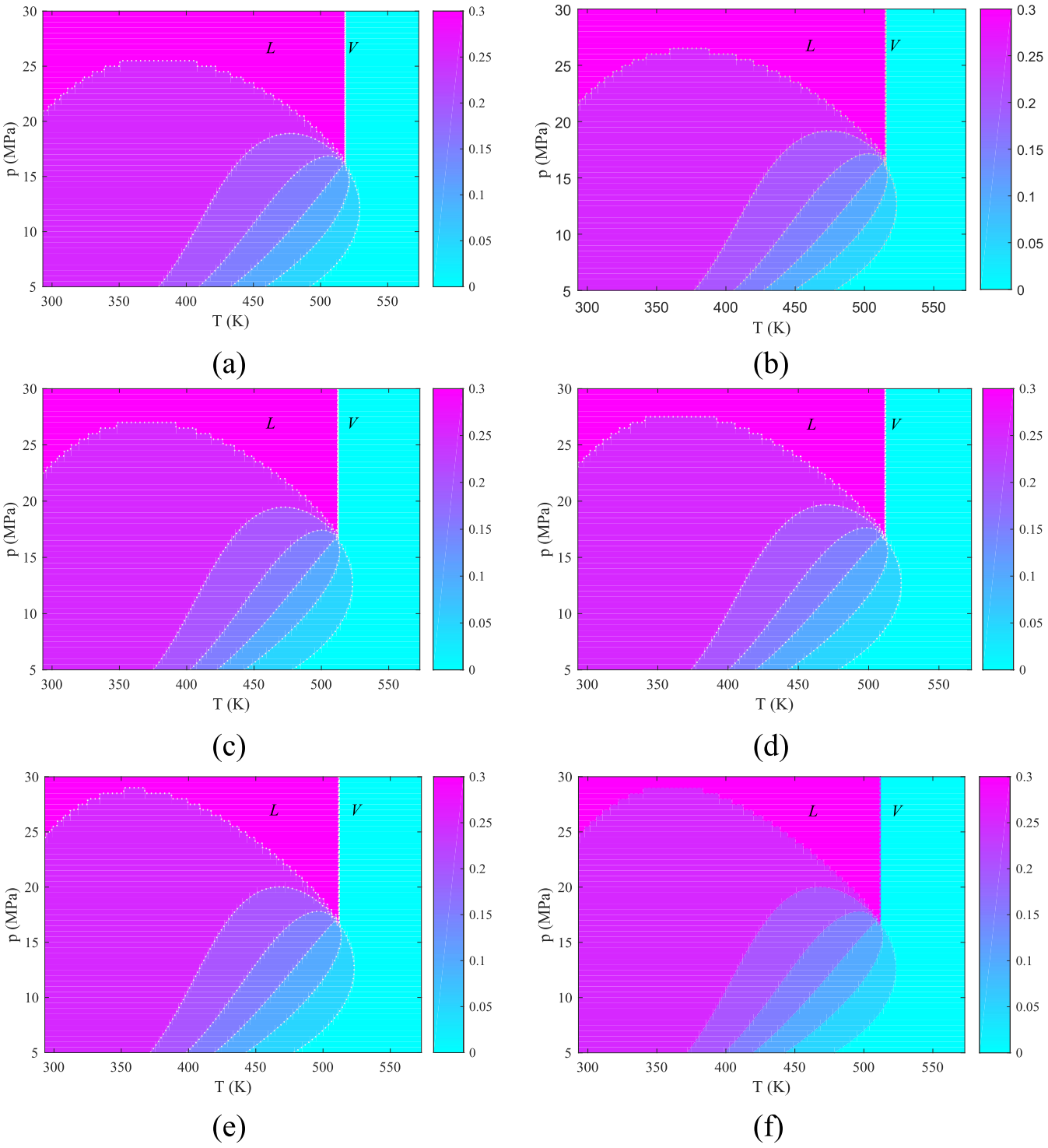

Figure 5. Liquid water distribution result (%). The corresponding salt content m_s in (a–f) is 0.001, 0.01, 0.02, 0.03, 0.05, and 0.1 mol, respectively.

For the liquid phase

$$(a\alpha)_m = \sum_i \sum_j [x_i x_j \sqrt{a_i a_j \alpha_i \alpha_j} \cdot (1 - k_{ij})], \quad b_m = \sum_i x_i b_i,$$

$$\psi_i = \sum_j [x_j \sqrt{a_i a_j \alpha_i \alpha_j} (1 - k_{ij})]$$

When brine exists in the system, the improved water component α coefficient and the binary interaction coefficient of introduced hydrocarbons and brine are expressed as[5]

$$\alpha = [1 + 0.4530[1 - T_r(1 - 0.0103c_{sw}^{1.1})] + 0.0034(T_r^{-3} - 1)]^2 \quad (4)$$

$$k_{iw} = (1.112 - 1.7369\omega_i^{-0.1})(1 + 0.017407c_{sw}) + (1.1001 + 0.836\omega_i)T_{ri}(1 + 0.033516c_{sw}) + (-0.15742 - 1.0988\omega_i)T_{ri}^2(1 + 0.011478c_{sw}) \quad (5)$$

https://doi.org/10.1021/acsomega.4c00223
ACS Omega 2024, 9, 20176−20184

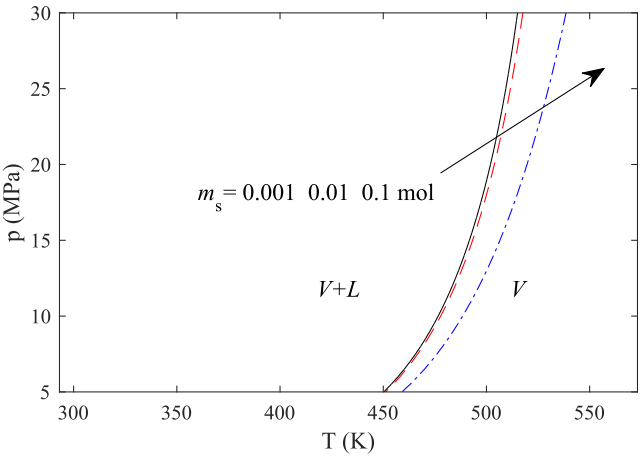

Figure 6. Phase diagram at different salt contents (C_1 and H_2O system).

Salinity is calculated based on the salt content and liquid water content

$$c_{sw} = \frac{m_s}{(m_s M_s + (1 - V)x_{H_2O}M_{H_2O})/1000} \quad (6)$$

According to the conservation of materials

$$V + L = 1 \quad (7)$$

$$Vy_i + Lx_i = z_i \quad (8)$$

$$\sum_i x_i = \sum_i y_i = 1 \quad (9)$$

Gas−liquid equilibrium conditions (equality condition of fugacity)

$$f_i^V = f_i^L \quad (10)$$

where

$$y_i = K_i x_i, f_i^V = \varphi_i^V y_i p, f_i^L = \varphi_i^L x_i p$$

Calculation Process. Phase equilibrium calculation can be completed by iterative solution of simultaneous equations. Different from the conventional phase equilibrium calculation, the salinity in the solution process also needs repeated iterative calculation. The process is shown in Figure 2. The salinity should be kept in the corresponding range at different temperatures. The maximum NaCl solubility in 100 g of water at different temperatures is shown in Table 1. Assuming that under initial conditions, the salt is soluble in water, the initial value of salinity can be defined as

$$c_{sw} = \frac{m_s}{(m_s M_s + z_{H_2O}M_{H_2O})/1000} \quad (11)$$

RESULTS AND DISCUSSION

Light hydrocarbons such as methane in natural gas are the main components, and the content of heavy hydrocarbons is less. Therefore, the two cases of considering heavy hydrocarbons and not considering heavy hydrocarbons are simulated correspondingly. First, the components in the simulation system include light hydrocarbon, heavy hydrocarbon, and water, and the molar percentage is 50, 20, and 30%, respectively. The effect of the salt content on the phase behavior is shown in Figure 3. When m_s = 0.001 mol, it can be considered that the salt content in the reservoir is very little or basically absent. It can be seen that the phase diagram changed greatly after considering the salinity. With the increase of the salt content in the system, the amount of dissolved salt in the liquid phase increases. The solubility of light hydrocarbons (methane) in the liquid phase decreases, and bubbles are prone to appearing in the liquid phase, resulting in an increase in the bubble point line. Therefore, the pressure range of the gas−liquid two-phase region increases. The increase of the salt content leads to the decrease of the temperature range in the gas−liquid two-phase region, and the critical temperature of the total system decreases. In addition, with the increase of the salt content, the dew point line in the phase diagram moves to the left and the dew point pressure gradually increases at the same temperature.

In the actual reservoir, the total amount of salt is constant. Under the same component content conditions, the reservoir salinity distribution curve with pressure and temperature is drawn, as shown in Figure 4. The salt is dissolved in liquid water, and the liquid water content can be calculated according to $L_{H_2O} = (1 - V)\cdot x_{H_2O}$. The calculation results are shown in Figure 5. Similar to the conventional phase diagram, the phase state can be distinguished by the envelope. In the pure liquid-phase region, the salinity and liquid water content are constant. Within the envelope, the salinity and its variation range decrease with the increase of the liquid water content. When the temperature gradually increases, the liquid water content decreases and tends to be saturated, and the salinity also increases sharply. After entering the vapor phase, there is no liquid water and all salt is precipitated.

When there are only 70% methane and 30% water in the system, the effect of the salt content on the phase behavior is shown in Figure 6. The critical parameters of methane and water are quite different, and it is difficult to see the parameters such as bubble point, dew point, and critical temperature from the phase diagram. However, the miscible region and the single-phase region can still be clearly distinguished by the envelope. The increase of the salt content will also expand the range of the gas−liquid two-phase region and shift the envelope line to the right. The salinity calculation results are shown in Figure 7. Similarly, the closer it is to the gas phase, the lesser the water in the liquid phase and the higher the salinity.

In order to reflect the relatively real phase characteristics of actual natural gas, considering the hydrocarbons and non-hydrocarbons in natural gas, the simulated components are redefined as shown in Table 2. The salt content m_s is 0.02 mol. The simulation results are shown in Figure 8. It can be seen from the contour lines in the figure that the gas percentage increases with an increase of temperature. The higher the temperature, the more obvious the effect of pressure on the gas percentage. Similarly, under high-temperature conditions, the percentage of liquid water, the percentage of water vapor, and the salinity change more obviously with pressure.

CASE STUDY

Selecting oilfield actual components for calculation: The formation pressure is 38.6 MPa and the reservoir temperature is 120 °C (393.15 K). The unit molar component in the reservoir contains 0.0211 mol of salt by fluid sampling. The fluid composition is shown in Table 3. The main components

https://doi.org/10.1021/acsomega.4c00223
ACS Omega 2024, 9, 20176−20184

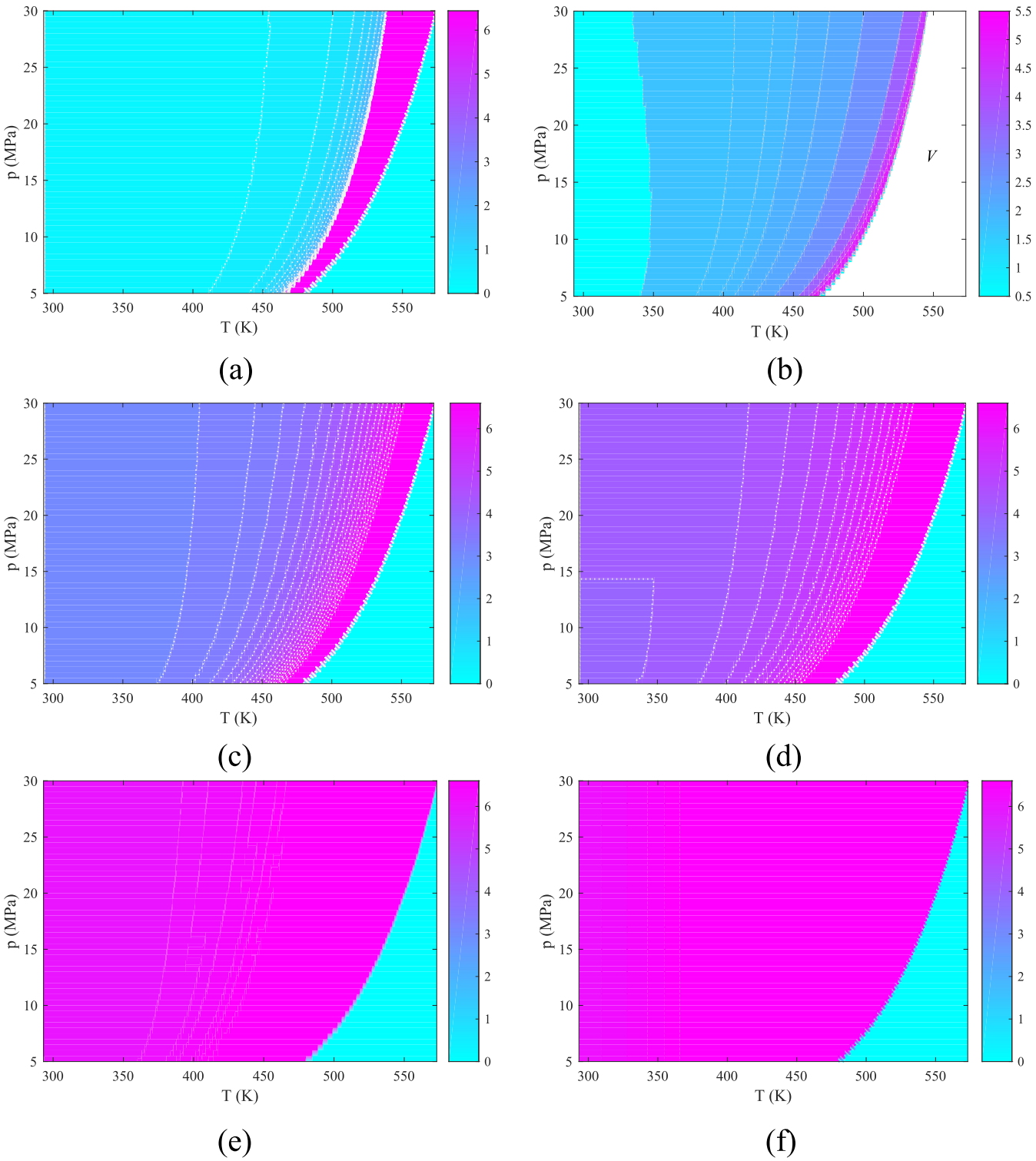

Figure 7. Salinity distribution result (mol/kg). The corresponding salt content m_s in (a−f) is 0.001, 0.01, 0.02, 0.03, 0.05, and 0.1 mol, respectively.

Table 2. Percentage of Fluid Components Simulated

component	mole (%)	component	mole (%)
C_1	0.58	CO_2	0.01
C_2	0.03	N_2	0.01
C_3	0.03	H_2S	0.01
C_4	0.03	H_2O	0.3

are methane and water with less heavy hydrocarbons. The phase diagram is shown in Figure 9. The corresponding salinity calculation results are shown in Figure 10. With the continuous exploitation of the reservoir, the formation pressure decreases and the temperature is relatively stable. The salinity variety with pressure is shown in Figure 11. As the pressure continues to drop, the percentage of gas (V) increases, the liquid water (V_{H_2O}) decreases, and therefore, the salinity (c_{sw}) increases. Until below the dew point pressure, the system is all gas; there

https://doi.org/10.1021/acsomega.4c00223
ACS Omega 2024, 9, 20176−20184

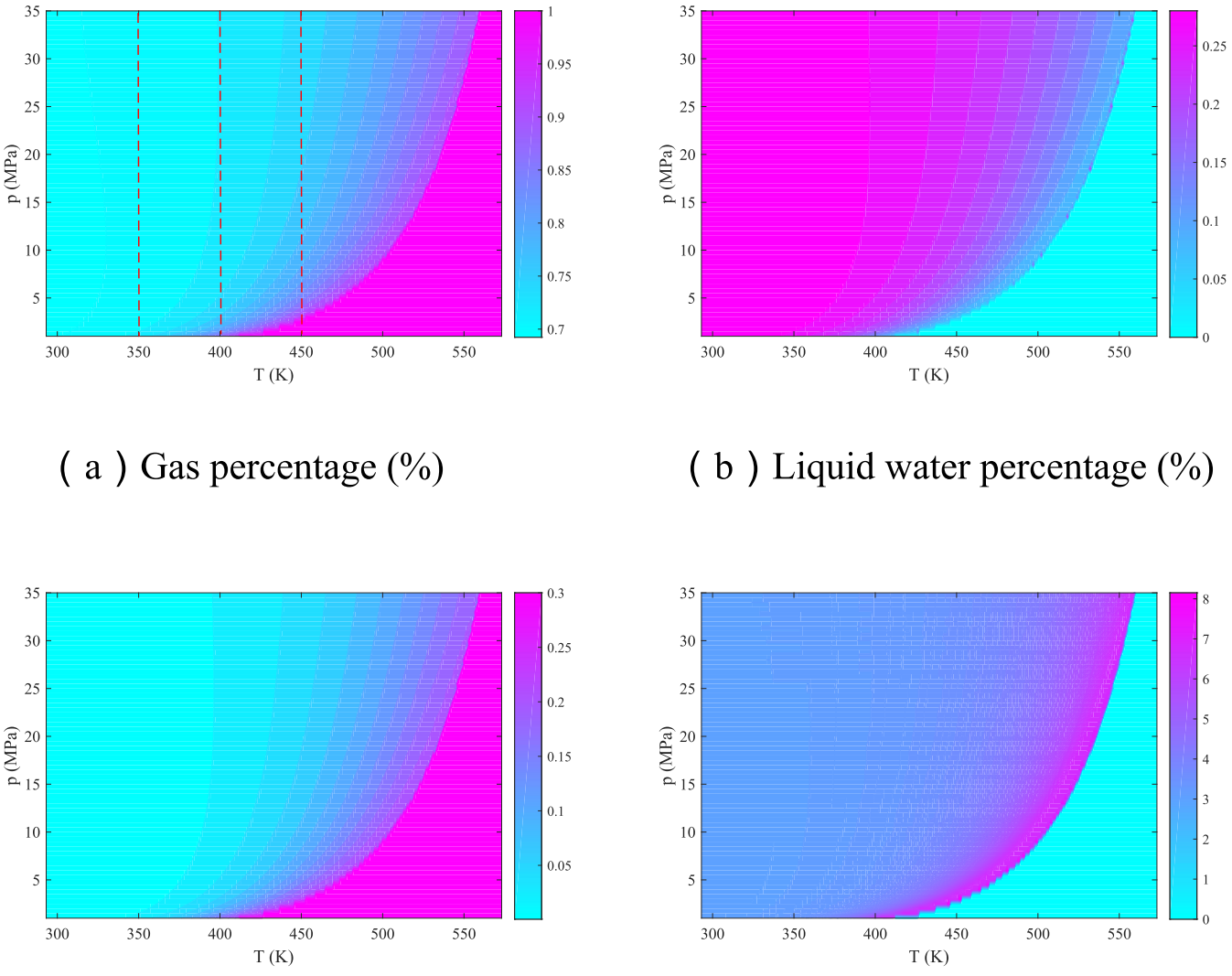

Figure 8. Fluid component percentage and salinity distribution results.

Table 3. Fluid Composition Percentage

component	mole (%)	component	mole (%)
C_1	0.7940	C_7	0.0013
C_2	0.0133	CO_2	0.0130
C_3	0.0024	N_2	0.0101
C_4	0.0013	H_2S	0.0182
C_5	0.0001	H_2O	0.1447
C_6	0.0016		

is no salinity. The dew point pressures at different temperatures can also be obtained from the phase diagram. For example, the dew point pressures at 393.15, 413.15, and 433.15 K are 1.08, 2.02, and 3.52 MPa, respectively. Then, guidance is provided for the reasonable control of the working system. According to the calculation results, the underground phase distribution and salinity variety can be monitored in real time. The calculation of fluid property parameters and reservoir parameters can be carried out subsequently.

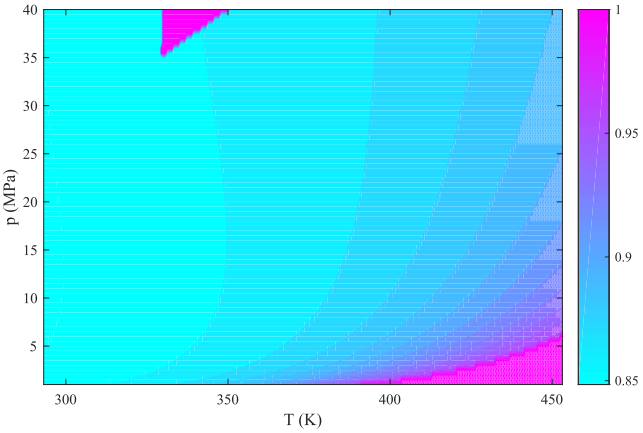

Figure 9. Measured phase diagram.

https://doi.org/10.1021/acsomega.4c00223
ACS Omega 2024, 9, 20176−20184

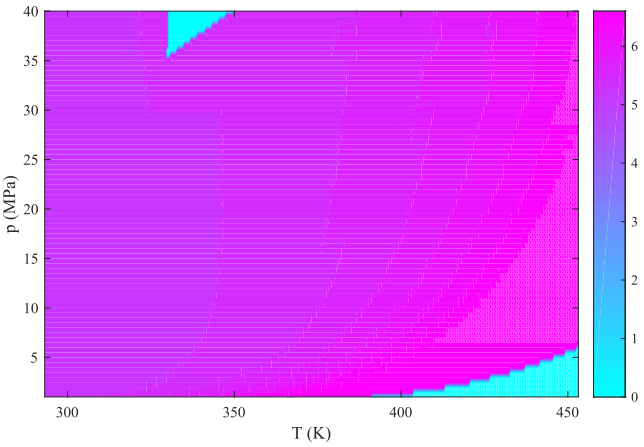

Figure 10. Salinity calculation results (mol/kg).

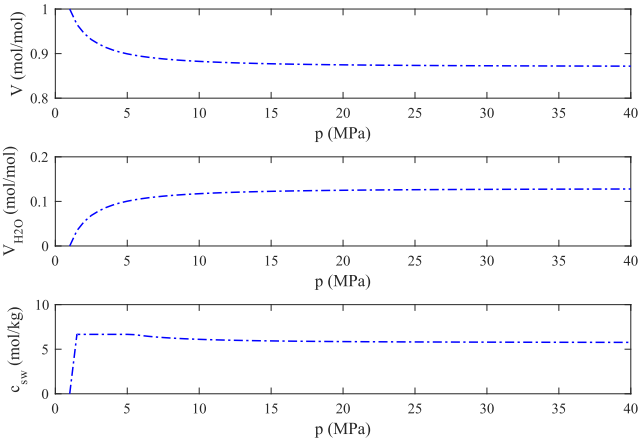

Figure 11. Gas percentage, liquid water percentage, and salinity variation curves (T = 393.15 K).

CONCLUSIONS

(1) The phase equilibrium calculation model of the hydrocarbon−water system considering salinity is established through introducing the binary interaction coefficient of hydrocarbon−salt water and α-function. In each iterative calculation process, the salinity is calculated according to the molar fraction of liquid water and salt contents. Compared with the conventional phase equilibrium calculation method, the number of iterations is increased. However, it can better reflect the real phase behavior characteristics of high-salinity reservoirs.

(2) The phase distribution under different salt contents and water contents was simulated. The salinity has a great influence on the phase behavior. After considering the salinity, the miscible zone in the phase diagram is expanded and the critical temperature is reduced. Similarly, the salinity calculation results can be obtained. With less liquid water, salinity rises sharply.

(3) The phase diagram was drawn by using the oilfield real component data, and the salinity calculation results were obtained. This method can realize the purpose of real-time monitoring of high-salinity reservoirs and provide a theoretical basis for a more realistic understanding of reservoir fluid properties.

AUTHOR INFORMATION

Corresponding Author

Zhongxin Ren − *China Oil & Gas Pipeline Network Corporation, Shanghai 200120, China;* orcid.org/0009-0006-3903-8841; Email: renzx01@pipechina.com.cn

Authors

Jianjun Li − *China Oil & Gas Pipeline Network Corporation, Shanghai 200120, China*

Hongfei Yuan − *Xi'an Sinoline Petroleum Science & Technology Co., Ltd., Xi'an 710065, China*

Chunxi Ai − *China Oil & Gas Pipeline Network Corporation, Shanghai 200120, China*

Hui He − *Xi'an Sinoline Petroleum Science & Technology Co., Ltd., Xi'an 710065, China*

Ken Qin − *China Oil & Gas Pipeline Network Corporation, Shanghai 200120, China*

Complete contact information is available at: https://pubs.acs.org/10.1021/acsomega.4c00223

Notes

The authors declare no competing financial interest.

ACKNOWLEDGMENTS

The authors would like to acknowledge the financial support from the Shaanxi Provincial Key R&D Plan Project-Oil and Gas Field Development Scheme Optimization Design Cloud Platform (No. 2019ZDLGY11-04).

NOMENCLATURES

c_{sw}	salinity, mol/kg
f_i	fugacity
K_i	gas−liquid equilibrium factor
k_{ij}	binary interaction coefficient
L	molar percentage of the liquid phase
L_{H_2O}	molar percentage of liquid water
M_{H_2O}	molecular weight of water, g/mol
M_s	molecular weight of salt, g/mol
m_s	mole number of salt per mole component in the system, mol
V	molar percentage of the gas phase
x_i	molar percentage of component i in the liquid phase
y_i	molar percentage of component i in the gas phase
z_i	molar percentage of component i in the total system
φ_i	fugacity coefficient
ω	acentric factor

REFERENCES

(1) Kutcherov, V. G.; Lopatin, A. S. Properties and phase behavior of Shtokman gas condensate at high pressure. *Pet. Sci. Technol.* **2019**, *37* (9), 1099−1105.

(2) Yin, B.; Li, X.; Qi, M. Study of Fluid Phase Behavior and Pressure Calculation Methods of a Condensate Gas Well. *Pet. Sci. Technol.* **2013**, *31* (16), 1595−1607.

(3) Li, Y.; Johns, R. T. In *Rapid Flash Calculations for Compositional Modeling*, SPE Annual Technical Conference and Exhibition, October 09; SPE: Dallas, Texas, 2005.

(4) Okuno, R.; Johns, R. T.; Sepehrnoori, R. Three-Phase Flash in Compositional Simulation Using a Reduced Method. *SPE J.* **2010**, *15* (3), 689−703.

(5) Mohebbinia, S.; Sepehrnoori, K.; Johns, R. T. Four-Phase Equilibrium Calculations of CO2/Hydrocarbon/Water Systems Using a Reduced Method. *SPE J.* **2012**, *18* (05), 943−951.

https://doi.org/10.1021/acsomega.4c00223
ACS Omega 2024, 9, 20176−20184

(6) Zhao, H. In *Flash Calculation and Phase Stability Analysis of Reservoir Gas-Water System-Implication for Extracting Dissolved CH_4 by CO_2 Injection*, SPE Annual Technical Conference and Exhibition, September 26; SPE: Dubai, UAE, 2016.
(7) Wyczesany, A. Calculation of Vapor−Liquid−Liquid Equilibria at Atmospheric and High Pressures. *Ind. Eng. Chem. Res.* **2014**, *53* (6), 2509−2519.
(8) Mikyška, J.; Firoozabadi, A. Investigation of mixture stability at given volume, temperature, and number of moles. *Fluid Phase Equilib.* **2012**, *321*, 1−9.
(9) Petitfrere, M.; Nichita, D. V. Robust and efficient trust-region based stability analysis and multiphase flash calculations. *Fluid Phase Equilib.* **2014**, *362*, 51−68.
(10) Smejkal, T.; Mikyška, J. Unifified presentation and comparison of various formulations of the phase stability and phase equilibrium calculation problems. *Fluid Phase Equilib.* **2018**, *476*, 61−88.
(11) Ma, X.; Wu, S.; Huang, G.; Fan, T. Three-Phase Equilibrium Calculations of Water/Hydrocarbon/Nonhydrocarbon Systems Based on the Equation of State (EOS) in Thermal Processes. *ACS Omega* **2021**, *6* (50), 34406−34415.
(12) Hinojosa-Gómez, H.; Solares-Ramírez, J.; Bazúa-Rueda, E. R. An improved algorithm for the three-fluid-phase VLLE flash calculation. *AIChE J.* **2015**, *61* (9), 3081−3093.
(13) Lindeloff, N.; Michelsen, M. L. Phase Envelope Calculations for Hydrocarbon-Water Mixtures. *SPE J.* **2003**, *8* (03), 298−303.
(14) Wang, K.; Luo, J.; Yan, L.; Wei, Y.; Wu, K.; Li, J.; Chen, F.; Dong, X.; Chen, Z. In *Artificial Neural Network Accelerated Flash Calculation for Compositional Simulations*, SPE Reservoir Simulation Conference, Galveston, March 29; SPE: Texas, USA, 2019.
(15) Zhao, H.; Jing, H.; Fang, Z.; Yu, H. Flash Calculation Using Successive Substitution Accelerated by the General Dominant Eigenvalue Method in Reduced-Variable Space: Comparison and New Insights. *SPE J.* **2020**, *25* (06), 3332−3348.
(16) Michelsen, M. L.; Yan, W.; Stenby, E. H. A Comparative Study of Reduced-Variables-Based Flash and Conventional Flash. *SPE J.* **2013**, *18* (05), 952−959.
(17) Ebadi, M.; Koroteev, D. In *Towards a Reliable Determination of Saturation Pressure: A Hybrid of Mouth Brooding Fish MBF Algorithm and Flash Calculations*, SPE/IATMI Asia Pacific Oil & Gas Conference and Exhibition, October 25; SPE: Bali, Indonesia, 2019.
(18) Paterson, D.; Michelsen, M. L.; Stenby, E. H.; Yan, W. In *New Formulations for Isothermal Multiphase Flash*, SPE Reservoir Simulation Conference, Montgomery, February 20; SPE: Texas, USA, 2017.
(19) Chempath, S.; Sun, H.; Haugen, K. In *Optimization Based Isenthalpic Flash for Thermal Reservoir Simulations*, SPE Reservoir Simulation Conference, February 20; SPE: Montgomery, Texas, USA, 2017.
(20) Han, C.; Chang, Y.-B.; Wolfsteiner, C.; Shi, X.; Schrader, M. In *A New Four-Phase Flash Algorithm for Surfactant Flood Simulation*, SPE Reservoir Simulation Conference, February 20; SPE: Montgomery, Texas, USA, 2017.
(21) Paterson, D.; Michelsen, M. L.; Stenby, E. H.; Yan, W. RAND-Based Formulations for Isothermal Multiphase Flash. *SPE J.* **2018**, *23* (02), 535−549.
(22) Neshat, S. S.; Okuno, R.; Pope, G. A. In *Simulation of Water and Condensate Blockage and Solvent Treatments in Tight Formations Using Coupled Three-Phase Flash and Capillary Pressure Models*, SPE Improved Oil Recovery Conference, April 14; SPE: Tulsa, Oklahoma, USA, 2018.
(23) Achour, S. H.; Okuno, R. In *Two-Phase Flash for Tight Porous Media by Minimization of the Helmholtz Free Energy*, SPE Improved Oil Recovery Conference, Virtual, August 30; SPE, 2020.
(24) Wang, S.; Sobecki, N.; Ding, D.; Wu, Y.-S.; Zhu, L. In *Accelerated Compositional Simulation of Tight Oil and Shale Gas Reservoirs Using Proxy Flash Calculation*, SPE Reservoir Simulation Conference, March 29; SPE: Galveston, Texas, USA, 2019.
(25) Sandoval, D.; Yan, W.; Michelsen, M. L.; Stenby, E. H. In *Phase Envelope Calculations for Reservoir Fluids in the Presence of Capillary Pressure*, SPE Annual Technical Conference and Exhibition, September 28; SPE: Houston, Texas, USA, 2015.
(26) Sun, H.; Li, H. Phase-Behavior Modeling of Hydrocarbon Fluids in Nanopores Using PR-EOS Coupled with a Modified Young−Laplace Equation. *ACS Omega* **2020**, *5* (25), 15177−15191.
(27) Mahiddini, A.; Tchouar, N.; Aguedal, H.; Ould-Kaddour, F.; Debab, A. Numerical prediction of phase equilibrium conditions of gas hydrates up to 200 MPa in the presence of sodium and calcium chloride solutions. *Pet. Sci. Technol.* **2022**, *40* (21), 2557−2570.
(28) Nichita, D. V. A volume-based approach to phase equilibrium calculations at pressure and temperature specifications. *Fluid Phase Equilib.* **2018**, *461*, 70−83.
(29) Nichita, D. V.; Petitfrere, M. Phase equilibrium calculations with quasi-Newton methods. *Fluid Phase Equilib.* **2015**, *406*, 194−208.
(30) Gernert, J.; Jäger, A.; Span, R. Calculation of phase equilibria for multicomponent mixtures using highly accurate Helmholtz energy equations of state. *Fluid Phase Equilib.* **2014**, *375*, 209−218.
(31) Petitfrere, M.; Nichita, D. V. Multiphase equilibrium calculations using a reduction method. *Fluid Phase Equilib.* **2015**, *401*, 110−126.
(32) Allahyarzadeh-Bidgoli, A.; Heidaryan, E.; Yanagihara, J. I.; de Alcântara Pessôa Filho, P. Assessment of correlations and simulation software to calculate phase diagrams of pre-salt fluids. *Pet. Sci. Technol.* **2021**, *39* (11−12), 410−420.
(33) Cui, G.; Ren, S.; Zhang, L.; Ren, B.; Zhuang, Y.; Li, X.; Han, B.; Zhang, P. Formation water evaporation induced salt precipitation and its effect on gas production in high temperature natural gas reservoirs. *Pet. Explor. Dev.* **2016**, *43* (05), 749−757.
(34) Gaidukov, L. A. In *Modeling of Wax and Salt Deposition in the Near-Well Zone of a Low-Temperature Reservoir Under Various Operating Conditions of Wells*, SPE Russian Petroleum Technology Conference, Virtual, October 26; SPE, 2020.
(35) Zhang, Y.; Isaj, E. In *Halite Envelope for Downhole Salt Deposition Prediction and Management*, SPE European Formation Damage Conference and Exhibition, June 03; SPE: Budapest, Hungary, 2015.

https://doi.org/10.1021/acsomega.4c00223
ACS Omega 2024, 9, 20176−20184